PHYSICAL REVIEW LETTERS

Li$^+$ Transport in Poly(Ethylene Oxide) Based Electrolytes: Neutron Scattering, Dielectric Spectroscopy, and Molecular Dynamics Simulations

Changwoo Do,[1,*] Peter Lunkenheimer,[2] Diddo Diddens,[3] Marion Götz,[2] Matthias Weiß,[2] Alois Loidl,[2] Xiao-Guang Sun,[4] Jürgen Allgaier,[5] and Michael Ohl[5]

[1]*Biology and Soft Matter Division, Oak Ridge National Laboratory, Oak Ridge, Tennessee 37831, USA*
[2]*Experimental Physics V, Center for Electronic Correlations and Magnetism, University of Augsburg, 86159 Augsburg, Germany*
[3]*Institut für Physikalische Chemie, Westfälische Wilhelms-Universität Münster, 48149 Münster, Germany*
[4]*Chemical Science Division, Oak Ridge National Laboratory, Oak Ridge, Tennessee 37831, USA*
[5]*Jülich Centre for Neutron Science, Forschungszentrum Jülich, 52425 Jülich, Germany*
(Received 19 November 2012; published 3 July 2013)

The dynamics of Li$^+$ transport in polyethylene oxide (PEO) and lithium bis(trifluoromethanesulfonyl) imde mixtures are investigated by combining neutron spin-echo (NSE) and dielectric spectroscopy with molecular dynamics (MD) simulations. The results are summarized in a relaxation time map covering wide ranges of temperature and time. The temperature dependence of the dc conductivity and the dielectric α relaxation time is found to be identical, indicating a strong coupling between both. The relaxation times obtained from the NSE measurements at 0.05 Å$^{-1} < q < 0.2$ Å^{-1} are of similar magnitude as the relaxation time of Li$^+$ predicted by MD simulation. Our results suggest that the characteristic live times of the ions within the oxygen cages are mainly determined by the α relaxation that corresponds to local segmental motions of polymers, to a much lesser extent by the main chain relaxation, and not at all by the β relaxation or other faster processes. It is the first time decisive experimental evidence for a microscopic picture of the Li ion transportation process is shown in which the PEO chain forms EO cages over several monomer units and the Li ion ''jump'' from cage to cage. The role of the backbone of the polymer is discussed and contributes signifcantly to the Li ion transportation process. Moreover, detailed characteristic length and time scales of the Li$^+$ transport process in this polymer electrolyte are identified and interpreted.

Lithium-ion batteries are commonly found in consumer electronics as various forms of portable devices or vehicles because of their high energy density, the absence of memory effects, and a slow loss of charge [1,2]. Rechargeable lithium-ion batteries based on solid polymer electrolytes (SPEs) offer many advantages over their liquid counterparts [3,4]. A major technical bottleneck, however, severely impedes the practical applications of SPEs in consumer electronics: the room-temperature conductivity is insufficient to power large portable devices [2,5,6]. Issues such as microscopic dynamics of lithium ions and their dependence on the polymeric matrix are known to play a key role in determining the ionic conductivity in SPEs. Therefore, understanding the microscopic dynamics of lithium ions embedded in a polymeric matrix is a crucial step for the interpretation of the ionic transport and toward the optimization of SPEs.

Polyethylene oxide (PEO) is one of the most widely studied polymers for the use of lithium-ion batteries due to its excellent salt-solvating ability. Although some studies show that the ion transport in the crystalline phase exceeds the ion conductivity of amorphous SPEs via tunneling [7], major efforts have been devoted to improve the conductivity of SPEs in the amorphous phase by reducing crystalline fractions of mixtures and by enhancing

segmental motions of polymers [8] and to finally understand the ion transport in relation to the segmental motion [9–12]. Mao *et al.* have observed two relaxation time scales of polymer dynamics in PEO:LiClO$_4$ and PEO: lithium bis(trifluoromethanesulfonyl)imde (LiTFSI) mixtures using quasielastic neutron scattering techniques -and attributed the fast and the slow motions to the dihedral-angle relaxation of PEO and the translational motion of chain segments, respectively [10,11]. The slowing down of the chain segment dynamics of PEO due to the bonding of Li$^+$ ions and oxygen atoms was observed and also supported by a separate neutron diffraction study [13] or computer simulations [14,15]. However, while neutron-scattering techniques have been unique probes to investigate the dynamics of polymers and demonstrated the strong correlation between segmental motions of polymers and the existence of Li$^+$ ions, only localized dynamics of polymers ($q > 0.8$ Å^{-1}) have been investigated so far and any correlation between large-scale polymer chain motions ($q < 0.2$ Å^{-1}) and Li$^+$ conductivity has not been fully exploited. Therefore, there still remains a missing link that bridges the long-time Li$^+$ transport property to the short-time segmental motions of polymers.

In the present study, we have investigated PEO:LiTFSI using different techniques such as NSE, as well as

dielectric spectroscopy and molecular dynamics (MD) simulations. NSE with isotope labeling techniques measures the dynamics in the low-q regime ($q < 0.2$ Å^{-1}) where normal-mode and segmental dynamics coexist. Dielectric spectroscopy, on the other hand, is dominated by segmental motions [16–18], and by the β relaxation [16]. MD simulation is used to describe experimentally inaccessible quantities such as the self-correlation function of Li$^+$ ions. We believe that our experimental and simulation results decisively demonstrate how the polymer chain motions at various length scales contribute to the Li$^+$ transport and establish the link between the long-time Li$^+$ transport properties and the short-time segmental motion of polymers.

The dynamic of various PEO samples was measured by neutron spin-echo (NSE) spectroscopy. The NSE experiments were performed, with and without LiTFSIs, with deuterated PEO molecules (dh-PEO) labeled at random positions along the chain (approximately 1 protonated monomer per 10 deuterated monomers). Polymer electrolytes were prepared by dissolving LiTFSI and PEO in acetonitrile and evaporating the solvent in a vacuum oven at 80 °C for 24 hr. NSE data of dh-PEO measured for samples with EO:Li = 10:1 and that without LiTFSI were collected. The ratio EO:Li = 10:1 was chosen to ensure a stable amorphous phase over a large temperature range, based on differential scanning calorimetry and small-angle neutron scattering (SANS) measurements [19]. While pure PEO was investigated at 400 K, for the EO:Li ratio 10:1 further temperatures between 400 and 450 K were collected. Figure 1(a) shows typical results measured at 450 K with an EO:Li ratio 10:1 pointing towards a relaxational process. However, at low Fourier
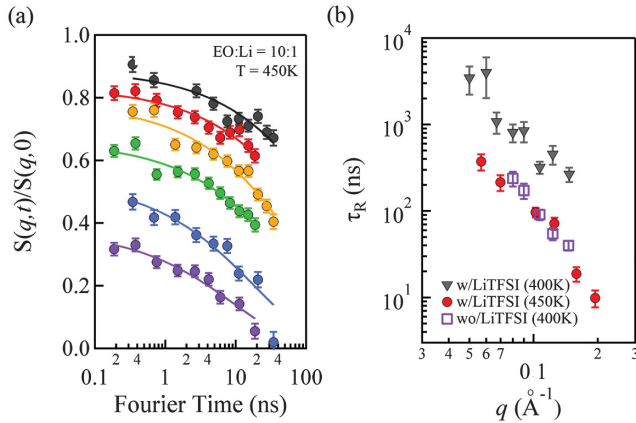

FIG. 1 (color). (a) NSE data (solid circles) of dh-PEO with LiTFSI (EO:Li = 10:1) at 450 K and fits (solid lines) using the KWW function with $\beta = 0.5$. NSE data of only a few selected q values ($q = 0.057$ Å^{-1}, 0.070 Å^{-1}, 0.125 Å^{-1}, 0.159 Å^{-1}, and 0.195 Å^{-1}, from top to bottom) are shown for clarity. (b) Characteristic relaxation times at various q values measured at $T = 400$ K and $T = 450$ K for PEO:LiTFSI = 10:1 and at $T = 400$ K for pure PEO.

times $S(q, t)/S(q, 0) \sim 1$ is not approached, even after proper normalization and background subtraction. This indicates the existence of an additional faster process that was also discussed in Ref. [11]. A Kohlrausch-Williams-Watts (KWW) function,

$$\frac{S(q, t)}{S(q, 0)} = A \exp\left[-\left(\frac{t}{\tau_R}\right)^{\beta}\right], \quad (1)$$

where A is the amplitude, β the shape parameter, and τ_R the relaxation time, was fitted to the experimental results. The shape parameter was fixed at values ranging from 0.4 to 0.6 and found to be of minor influence on the time scales derived from fits to the KWW function. For the segmental relaxation or α relaxation, the shape parameter also remained within this reasonable range from 0.35 to 0.55 when q was varied from 0.8 Å^{-1} to 1.6 Å^{-1} [11]. Therefore, also following the suggestion from Ref. [20], the shape parameter was fixed to $\beta = 0.5$. It has to be noted that our PEO samples were prepared by mixing partially deuterated PEOs with fully deuterated PEOs in order to increase miscibility of two kinds of PEOs with different scattering length density. Therefore, in addition to the self-correlation function of the EO segment, the normal mode of the PEO chain is also measured at a chosen momentum transfer. It is expected that in the present experiments the segmental relaxation is not detected, especially at the lowest momentum transfer, since the length scales corresponding to the covered q range are much larger. The time scales resulting from the KWW fits will be discussed again later in the overall relaxation map. Obviously, the relaxation that we detect in the NSE measurements is much slower than the segmental and other relaxations reported elsewhere [10,21]. Thus, one can assume that the normal mode might be responsible for the dynamics revealed in these spectra [22].

From a comparison with the relaxations times obtained for pure PEO [Fig. 1(b)], it is very clear that τ_R for PEO with LiTFSI is increased approximately by an order of magnitude, indicating that the detected dynamics dramatically slows down by the addition of ions. For q ranges >0.2 Å^{-1}, there have been several reports of slowing down of the PEO dynamics in the presence of Li salts [10,11]. However, at low q ranges where the dynamics on a larger scale up to ~10 nm is observed, the effect of Li$^+$ on chain dynamics has not yet been fully investigated. Figure 1(b) shows the q dependence of τ_R as obtained from the fits shown in Fig. 1(a). As it can be seen from the SANS data [19], the scattering intensity at $q < 0.2$ Å^{-1} is dominated by coherent scattering. In our experimental conditions, coherent single-chain form factors are expected since 30 wt % of PEO chains have randomly protonated monomers (of 30 wt %). Therefore, in Fig. 1(b) the characteristic relaxation times reaching up to hundreds of nanoseconds at $q < 0.2$ Å^{-1} can be attributed to the normal mode of PEO chains, which describes the large length scale

(>3 nm) dynamics. Above $q \sim 0.2$ Å^{-1}, the scattering
intensities are dominated by the incoherent background
from the protonated monomers. Therefore, the self-
correlation functions of monomers are measured by NSE,
in other words, segmental motions of monomers. In this
high-q region, τ_R of pure PEO is consistent with the
previously reported values by Brodeck *et al.* [20] using
incoherent intermediate scattering techniques, which cover
higher q values (0.2 Å$^{-1} \leq q \leq 2.0$ Å^{-1}).

While, in NSE, the observed relaxation features arise
from mixtures of local segmental motions and chain
normal modes, the segmental relaxation behavior was
independently investigated using dielectric measurements.
Dielectric measurements directly couple to both the dipo-
lar degrees of freedom and the Li-ion transport in PEO,
whose dynamics can be investigated in a wide frequency
and temperature range. For the present work, we have
studied the sample with a PEO:LiTFSI ratio of 10:1 at
frequencies from 1 Hz to 1 GHz and at temperatures from
150 to 350 K [19]. Figure 2 shows the α and β relaxation
times obtained from the fits to the measured dielectric
constant and conductivity data, significantly extending
the temperature range of the relaxation time data reported
in Ref. [17]. In addition, the dc resistivity ρ_{dc}, deduced
from the dielectric measurements, is shown (crosses).
It reasonably agrees with the results of the independently
measured dc conductivity [19]. In literature, often a close
correlation of segmental motion and ionic charge transport
is assumed [3,17,23]. Thus, the $\rho_{dc}(T)$ plot (right scale of
Fig. 2) was scaled to achieve the same number of decades
per cm as for the $\tau(T)$ plots (left scale) and vertically
shifted to match the $\tau_\alpha(T)$ curve. Obviously, $\rho_{dc}(T)$ and
$\tau_\alpha(T)$ exhibit nearly identical temperature dependence.
The solid line in Fig. 2 represents a fit of $\tau_\alpha(T)$ with
the phenomenological Vogel-Fulcher-Tammann (VFT)
equation [24–26],

$$\tau = \tau_0 \exp\left[\frac{D T_{VF}}{T - T_{VF}} \right]. \qquad (2)$$

Here τ_0 is an inverse attempt frequency, D is the so-called
strength parameter, and T_{VF} is the Vogel-Fulcher tempera-
ture. The obtained fit curve ($\tau_0 = 3.8 \times 10^{-13}$ s, $D = 8.0$,
and $T_{VF} = 177$ K) provides a good description of the
relaxation-time data and, moreover, a reasonable match
of the dc resistivity data is achieved. Thus, these results
indicate that the ionic charge transport in PEO-LiTFSI is
indeed strongly coupled to the α process (which in poly-
mers corresponds to the segmental motion), as also often
found for electrolyte solutions and dipolar glass-forming
liquids [27] and as also predicted by the Debye-Stokes-
Einstein relation. This can be easily rationalized if regard-
ing the ionic charge transport as the motion of spheres
through a viscous medium and if having in mind that it is
the α relaxation that determines the viscosity. However, the
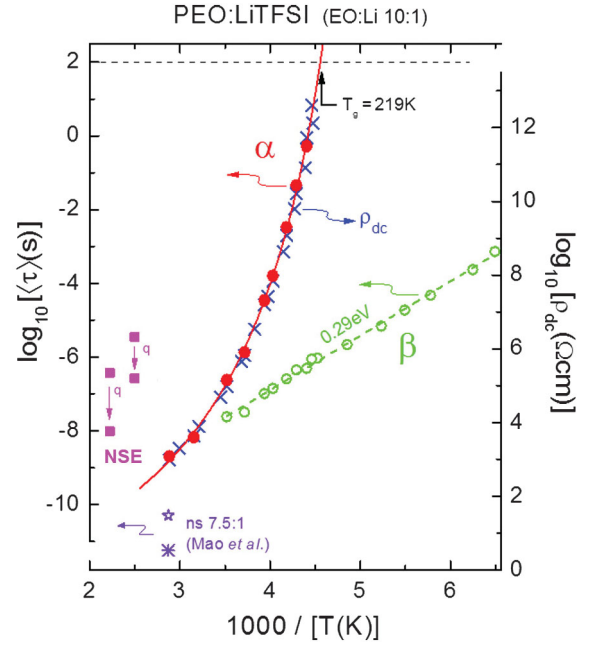rigidity of the polymer chain also has to be accounted for as

FIG. 2 (color).   Arrhenius diagram showing the relaxation time
map (left scale) and the dc resistivity (right scale). The relaxation
time constants from NSE (squares) are shown for the lowest (upper
data point) and highest values of q (lower point). The α (closed
circles) and β relaxation times (open circles) were determined
from fits of the dielectric spectra [19]. The solid line shows a fit of
the α relaxation time with the VFT equation. The dashed line is a
fit of $\tau_\beta(T)$ with an Arrhenius law revealing an energy barrier of
0.29 eV. The dc resistivity curve is vertically shifted to match the α
relaxation times, demonstrating a perfect agreement of the tem-
perature dependences of both quantities (note the same decades/
cm scaling of both ordinates). The stars denote the relaxation times
reported in the work by Mao *et al.* [10] for an EO/Li ratio of 7.5/1
(we show an approximate q-averaged value, read off from the
dashed lines in Fig. 3 of Ref. [10]).

it was recently shown for a series of PEO-related polymer
electrolytes [28]. Figure 2 also shows the relaxation time
τ_R from the present NSE measurements at the lowest
and highest of q values, measured at two temperatures
(squares). They are several decades larger than those of
the segmental α relaxation, fully consistent with their
interpretation as normal modes. Comparison of the
obtained normal-mode time scales with those associated
with the ionic charge transport at corresponding length
scales of NSE indicates that this relaxational process is
also correlated with the ionic charge transport in PEO at
macroscopic length scales [19]. The dielectric data also
revealed the presence of a secondary β process that follows
an Arrhenius law with activation energy of 0.29 eV (Fig. 2,
open circles and dashed line). In Ref. [23], the β relaxation
in PEO:LiTFSI was proposed to arise from the local reor-
ientation of the C-O bond dipoles in the polymer chain.
However, it should be noted that secondary relaxations
in polymers are also often identified with the so-called
Johari-Goldstein relaxation [29], which was shown to arise

in numerous glass forming materials and are believed to be an inherent property of glassy matter [18,29–31]. In any case, this secondary process detected in PEO:LiTFSI does not seem to play a role in the conductivity process of the Li^+ ions.

Based on the identical temperature-dependent behavior of resistivity with α relaxation time (Fig. 2) and the good agreement of time scales from NSE and conductivity at a given length scale ($q \sim 0.1$ Å^{-1}; see the Supplemental Material [19]), we conclude that the Li^+ transport is greatly assisted by the local segmental motion of the polymer and by the normal mode of polymer chains at large length scales. Our observations also lead to a consistent view with existing literatures [10,11,13], where cage trapping and hopping processes are suggested. However, direct observation of such trapping and hoping dynamics of Li^+ cannot be easily accessed by experimental techniques. Therefore, MD simulation was performed to further enhance our understanding of the Li^+ transport mechanism.

The intermediate scattering functions calculated from the MD simulations and their analysis are described in detail in the Supplemental Material [19]. In Fig. 3(a), indexes of oxygen atoms within a PEO chain interacting with Li^+ are plotted over a time of 15 ns. At any given time, more than one oxygen atom typically is coordinated with the Li^+ ion [Fig. 3(b)]. It is interesting to see that distinctive time regions can be identified [shown with shaded regions in Fig. 3(a)], where the coordination indexes are clearly separated. At early simulation times (4–8 ns), Li^+ ions are associated with the oxygen atoms of index 5 to 11, while the oxygen atoms of index 12 to 17 are dominantly associated with Li^+ at later times (after ~8 ns). This suggests that the Li^+ ion spends approximately 4–7 ns within the cage and the hopping process to the next cage occurs much faster, within time scales of 1 ns. The interchain hopping process was also captured from the MD trajectory [Fig. 3(c)]. Here, the observed transition time during which both PEO chains share one Li^+ ion is less than 1 ns. The trajectory of Li^+ at every 100 ps is plotted in a three-dimensional box with projections onto the x-y plane [Fig. 3(d)]. A few localized regions, separated by 10–20 Å distances, with high density of Li^+ coordinates can be identified, which also supports the cage-hopping transport process of Li^+. The diffusion coefficients (6.55 Å^2/ns and 11.18 Å^2/ns for 400 and 450 K) calculated from the Li^+ conductivity values of the simulation [15,19] agree very well with the diffusion coefficients derived from the experimentally deduced conductivities (6.4 Å^2/ns and 13.9 Å^2/ns; see the Supplemental Material [19] for detailed calculation). The close agreement indicates that the local dynamic picture of caging and hopping of Li^+ as revealed by the MD simulations is reliable. The trapping time as observed in Fig. 3(a), therefore, can be responsible for the relatively slow macroscopic
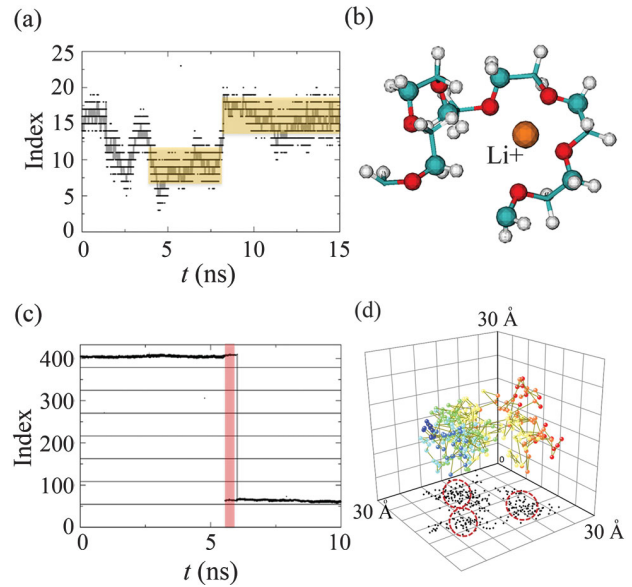

FIG. 3 (color). (a) Index of oxygen atoms of a PEO chain interacting with a Li^+ ion at time t, representing the intrachain hopping process. Gray line is an average at each time. Shaded areas indicate cages formed at different times. (b) Snapshot of MD simulation showing a Li^+ caged by a PEO chain. (c) Index of oxygen atoms from all oxygens in the simulation box interacting with a Li^+ ion at time t, representing an interchain hopping process. The gray vertical line at 6 ns indicates the moment of completed transition from one cage to another cage of different PEO chains. Shaded area indicates the transition time of less than 1 ns. (d) Li^+ trajectory plotted every 100 ps during 30 ns. Projected coordinates are shown in the x-y plane to help with visualization. Higher density of coordinate points indicates Li^+ trapped in the cage of oxygens (dashed red circles).

Li^+ transport, even though the segmental motion of the cages are much faster and exhibit similar temperature dependencies (Fig. 2).

We identified individual contributions of different dynamics processes to the macroscopic Li^+ transport. The NSE measurements revealed a dramatic slowing down of the detected relaxation mode in the presence of LiTFSI and the contribution of segmental motion and normal mode at different length scales. The temperature dependence of the dc conductivity and the dielectric α relaxation time is found to be identical, indicating a strong coupling between both. The characteristic live times of Li^+ within the cages formed by PEO chains are mainly determined by the segmental α relaxation and the main chain relaxation, and not at all by the β relaxation or any other faster processes. The fast hopping process from one cage to another plays a significant part in macroscopic conductivity and is found to be the fastest transport process. The significant contribution of the hopping process also explains the high mobility of Li^+ ions in some of the crystalline phases of PEO mixtures reported so far [7] and is also in line with the recent findings by Wang *et al.*, relating the decoupling of segmental motion and ion

mobility to frustration in the packing of rigid polymers [28]. The diffusion time scale estimated from the ion conductivity agrees excellently with the relaxation time scale measured by NSE at corresponding length scales and also is consistent with the results from MD simulations supporting that our understanding on Li^+ transport is reasonable. To summarize, we were able to show, for the first time, decisive experimental evidence for Li ion transportation undergoing a "jump" process from EO cages formed by several monomer units of the PEO chain. The role of the backbone was discussed and astonishingly plays a major role of the Li ion transportation as well. Detailed lengths and time scales have been determined and deliver valuable information for future applications and design of new materials.

*doc1@ornl.gov

[1] E. Peled, *Lithum Batteries* (Academic, New York, 1983).

[2] J. B. Goodenough and Y. Kim, Chem. Mater. **22,** 587 (2010).

[3] F. Croce, G. B. Appetecchi, L. Persi, and B. Scrosati, Nature (London) **394,** 456 (1998).

[4] A. M. Stephan and K. S. Nahm, Polymer **47,** 5952 (2006).

[5] J. M. Tarascon and M. Armand, Nature (London) **414,** 359 (2001).

[6] A. S. Arico, P. Bruce, B. Scrosati, J. M. Tarascon, and W. V. Schalkwijk, Nat. Mater. **4,** 366 (2005).

[7] Z. Gadjourova, Y. G. Andreev, D. P. Tunstall, and P. G. Bruce, Nature (London) **412,** 520 (2001).

[8] S. K. Fullerton-Shirey and J. K. Maranas, J. Phys. Chem. C **114,** 9196 (2010).

[9] P. G. Bruce and C. A. Vincent, J. Chem. Soc., Faraday Trans. **89,** 3187 (1993).

[10] G. M. Mao, R. F. Perea, W. S. Howells, D. L. Price, and M. L. Saboungi, Nature (London) **405,** 163 (2000).

[11] G. Mao, M.-L. Saboungi, D. L. Price, M. Armand, F. Mezei, and S. Pouget, Macromolecules **35,** 415 (2002).

[12] S. K. Fullerton-Shirey and J. K. Maranas, Macromolecules **42,** 2142 (2009).

[13] G. M. Mao, M. L. Saboungi, D. L. Price, M. B. Armand, and W. S. Howells, Phys. Rev. Lett. **84,** 5536 (2000).

[14] F. Müller-Plathe and W. F. v. Gunsteren, J. Chem. Phys. **103,** 4745 (1995).

[15] O. Borodin and G. D. Smith, Macromolecules **39,** 1620 (2006).

[16] M. Marzantowicz, J. R. Dygas, F. Krok, Z. Florjanczyk, and E. Zygadlo-Monikowska, J. Non-Cryst. Solids **352,** 5216 (2006).

[17] M. Marzantowicz, J. R. Dygas, F. Krok, Z. Florjanczyk, and E. Zygadlo-Monikowska, J. Non-Cryst. Solids **353,** 4467 (2007).

[18] F. Kremer and A. Schönhals, *Broadband Dielectric Spectroscopy* (Springer, Berlin, 2002).

[19] See Supplemental Material at http://link.aps.org/supplemental/10.1103/PhysRevLett.111.018301 for details of experimental methods and data from differential scanning calorimetry, SANS, dielectric spectroscopy, and MD simulation.

[20] M. Brodeck, F. Alvarez, A. Arbe, F. Juranyi, T. Unruh, O. Holderer, J. Colmenero, and D. Richter, J. Chem. Phys. **130,** 094908 (2009).

[21] M. Brodeck, F. Alvarez, J. Colmenero, and D. Richter, Macromolecules **45,** 536 (2012).

[22] K. E. Shuler, *Stochastic Processes in Chemical Physics* (John Wiley & Sons Interscience, New York, 1969).

[23] J. P. Donoso, T. J. Bonagamba, H. C. Panepucci, L. N. Oliveira, W. Gorecki, C. Berthier, and M. Armand, J. Chem. Phys. **98,** 10026 (1993).

[24] G. S. Fulcher, J. Am. Ceram. Soc. **8,** 339 (1925).

[25] G. Tammann, W. Hesse, and Z. Anorg, Z. Anorg. Allg. Chem. **156,** 245 (1926).

[26] H. Vogel, Z. Phys. **22,** 645 (1921).

[27] M. Köhler, P. Lunkenheimer, and A. Loidl, Eur. Phys. J. E **27,** 115 (2008).

[28] Y. Wang, A. L. Agapov, F. Fan, K. Hong, X. Yu, J. Mays, and A. P. Sokolov, Phys. Rev. Lett. **108,** 088303 (2012).

[29] G. P. Johari and M. Goldstein, J. Chem. Phys. **53,** 2372 (1970).

[30] P. Lunkenheimer, U. Schneider, R. Brand, and A. Loidl, Contemp. Phys. **41,** 15 (2000).

[31] S. Kastner, M. Köhler, Y. Goncharov, P. Lunkenheimer, and A. Loidl, J. Non-Cryst. Solids **357,** 510 (2011).